Aberration Correction With OFF: The Overdetermined, Fan-Filtering Algorithm

Mark A. Haun, Douglas L. Jones, and William D. O'Brien, Jr.

Department of Electrical and Computer Engineering
University of Illinois at Urbana-Champaign, Urbana, IL 61801

Abstract — As medical ultrasound imaging moves to larger apertures and higher frequencies, tissue sound-speed variations continue to limit resolution. In geophysical imaging, a standard approach for estimating near-surface aberrating delays is to analyze the time shifts between common-midpoint signals. This requires complete data—echoes from every combination of an individual source and receiver. Unfocused, common-midpoint signals remain highly correlated in the presence of aberration; there is also tremendous redundancy in the data.

In medical ultrasound, this technique has been impaired by the wide-angle, random-scattering nature of tissue. Until now, it has been difficult to estimate azimuth-dependent aberration profiles or to harness the full redundancy in the complete data. Prefiltering the data with two-dimensional fan filters largely solves these problems, permitting highly overdetermined, least-squares solutions for the aberration profiles at many steering angles. In experiments with a tissue-mimicking phantom target and silicone rubber aberrators at nonzero stand-off distances from a 1-D array transducer, this overdetermined, fan-filtering algorithm (OFF) significantly outperformed other published algorithms.

1. BACKGROUND

Many algorithms have been proposed for aberration correction in medical ultrasound imaging. Those which would be practical *in vivo* are generally based on a screen model. In it, the aberration is modeled entirely by variable time delays on the received and transmitted signals due to an infinitesimally thin screen at the transducer surface; these delays are known as the aberration profile. If the aberration profile can be estimated correctly, focusing is easily accomplished by adding compensating delays to the hyperbolic focusing operators dictated by geometry. For a one-dimensional array transducer at $z = 0$ scanning in the x-z (azimuth) plane (Fig. 1),

$$\tilde{t}_k(x', z') = t_k(x', z') + \tau_k \quad (1)$$

$$= \frac{1}{c}\sqrt{(x_k - x')^2 + z'^2} + \tau_k. \quad (2)$$

Supported by the University of Illinois Research Board and NIH CA79179.
Email correspondence to markhaun@uiuc.edu.

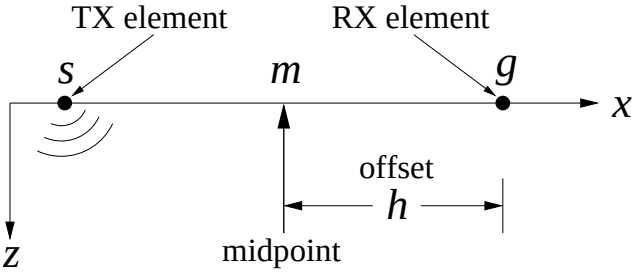

Figure 1: A simple reflection experiment defining the positions of transmit element s, receive element g, midpoint m, and offset h.

Here, x_k is the position of the k-th array element, and (x', z') is the target location. For a constant sound speed c, the one-way travel times $\{t_k\}$ define a hyperbola in the (x, t) space of the recorded data. These may be viewed as a focusing operator for the point (x', z'), where the array elements are fired at times $\{-t_k\}$ for transmit focusing, the reflection occurs at time zero, and the received echoes are coherently combined at times $\{t_k\}$ for receive focusing [1]. The aberration profile, $\{\tau_k\}$, is added to $\{t_k\}$ to form $\{\tilde{t}_k\}$, the correct focusing operator in the presence of aberration.

While a single screen model does not describe the distributed aberration found in tissue, a single aberration profile may be acceptable for a small part of the image—an isoplanatic patch. By calculating many aberration profiles, the entire image may be corrected.

One approach to aberration correction in medical ultrasound imaging exploits the redundant information contained in "complete" data [2,3]. A complete data set $d_{s,g}(t)$ has N^2 signals, one for every possible combination of an individual source s and receiver g in an N-element array. These data are highly redundant; in particular, the common-midpoint signals $d_{m-h,m+h}(t)$, with m constant, are highly correlated. This makes them attractive for estimating aberration profiles and suggests ordering the data by midpoint-offset (m-h) coordinates (Fig. 1).

Algorithms based on common-midpoint signal analysis are less susceptible to misconvergence than those requiring an initial transmit focus, because common-midpoint signals remain highly correlated even in the presence of aberration.

The process of transmit focusing (summing $d_{s,g}(t)$ over s) assumes knowledge of the correct focusing operator; if this assumption is incorrect, useful information is irretrievably lost. When signals are analyzed prior to focusing, the extra information can be used to derive a more robust solution—in theory, $\approx N^3/12$ equations in N unknowns [6].

Time shifts between common-midpoint signals derive not only from aberration, but also from the source-receiver separation and the location of the reflecting target(s). If the aberrating delays are to be estimated accurately, the latter two effects must be properly accounted for. Consider the travel time t versus offset h for reflections from a flat reflector at depth z':

$$t = \frac{2}{c}\sqrt{\left(\frac{g-s}{2}\right)^2 + z'^2} = \frac{2}{c}\sqrt{h^2 + z'^2}. \qquad (3)$$

In the seismic imaging community, this hyperbolic dependence on offset is called *normal moveout*, or NMO, and leads to the NMO correction whose purpose is to flatten the hyperbolas on common-midpoint signal sets [4]. This may precede summation over offset to reduce noise, or, in our case, cross-correlations between signals at different offsets to estimate the aberration profile.

Flat reflectors are rare in medical ultrasound imaging, and reflection energy typically returns to the transducer from many directions simultaneously. Thus, NMO correction was extended to angles away from the array normal ($\theta \neq 0°$) [3]. This generalized moveout correction defines the change of variable $t \rightarrow t'$, where

$$t' = \sqrt{\frac{t^2}{4} + \frac{h^2}{c^2} - t\frac{h}{c}\sin\theta} + \sqrt{\frac{t^2}{4} + \frac{h^2}{c^2} + t\frac{h}{c}\sin\theta}. \quad (4)$$

By itself, this does nothing to suppress echoes coming from azimuths other than θ. In the no-aberration case, all reflections on the corrected common-midpoint signal sets should be perfectly flat (t' independent of offset h). Echoes from off-axis, however, will not be straightened out, leading to an undesirable bias in the time-shift estimates. The moveout correction grows rapidly with increasing offset, and so does the bias from uncorrected, off-axis scatterers. The lack of directionality in the processing is actually a compound problem: First, even if the aberration profile is not θ-dependent, bias in the time-shift estimates will perturb the solution. Second, the aberration usually **is** θ-dependent!

In [3], time-shift estimation bias is largely avoided by considering only time shifts between signals of offset 0 and 1 element. The resulting set of $N-2$ equations is sufficient to find the aberration profile to within an unknown linear tilt, but the algorithm has to ignore the wealth of redundant information contained in the longer offsets. Furthermore, it has difficulty finding different aberration profiles at different azimuth angles when used with a small-element array. An updated version [5] uses focused subarrays to achieve some directionality. Unfortunately, this reduces the resolution of the estimated profiles and still precludes the use of a large offset spread to achieve a robust, overdetermined system. In the following section, the directionality problem is addressed in a new way using two-dimensional fan filters.

2. Angle preselection using 2-D fan filters

Consider a point source located at (x', z'), representing the reflection from a point target at time zero. Using continuous functions for simplicity, let $p(t)$ be the transmitted pulse and $\tau(x)$ the aberration profile. Neglecting amplitude factors, the aberrated signal received across the array is

$$\tilde{d}(x,t) = p\left[t - \frac{1}{c}\left((x-x')^2 + z'^2\right)^{1/2} - \tau(x)\right]. \quad (5)$$

Fourier transforming in time yields $\tilde{D}(x,F)$; then, noting that only the phase of $\tilde{D}(x,F)$ depends on x, the instantaneous spatial frequency F_x may be found from the derivative of this phase with respect to x. For the case of no aberration,

$$F_x = -\frac{F}{c}\frac{x-x'}{\left((x-x')^2 + z'^2\right)^{1/2}} = \frac{F}{c}\sin\rho \qquad (6)$$

where ρ is the angle made by the aperture-to-reflector line with respect to the z-axis. Thus, the unaberrated spectrum from a point target is contained within the fan-shaped regions determined by the temporal bandwidth and the spatial extent of the aperture [6].

Now suppose that time-shift aberration is present. Letting $\tilde{D}$ and D denote the received signals' 2-D spectra in the aberrated and unaberrated cases, respectively, application of the frequency-convolution property yields

$$\tilde{D}(F_x, F) = D(F_x, F) * U(F_x, F) \qquad (7)$$

where

$$U(F_x, F) = \mathcal{F}_x\left[e^{-j2\pi F\tau(x)}\right] \qquad (8)$$

and the convolution is in F_x. The effect of aberration, then, is to convolve the original spectrum in spatial frequency with that of a phase-modulated signal. The spreading effect in F_x is proportional to the rms amplitude of the aberration and inversely proportional to its correlation length [6]. Simulations and experiments with typical expected aberration profiles have shown that despite this effect, digital fan filters defined by (6) are effective at targeting particular image regions for common-midpoint signal analysis.

Fig. 2 presents the overdetermined, fan-filtering algorithm (OFF), a practical implementation of this approach. See [6] for an in-depth discussion of each step. For the results presented next, $\Delta\rho$ was 10 degrees and x_{thresh} was 0.5. The offset range h_{min} to h_{max} was 1 to 12 elements.

3. EXPERIMENTAL RESULTS

Complete data sets were acquired in the Bioacoustics Research Laboratory at the University of Illinois using a 1-D, 64-element transducer (2.6-MHz center frequency, 315-μm pitch) and a custom data-acquisition system [6]. Artificial 1-D aberrating structures were constructed from GE RTV615. This material has an 1100-m/s speed of sound and an acoustic impedance similar to that of soft tissue, providing strong refraction without much reverberation. The aberrators were interposed between the transducer and a tissue-mimicking phantom (ATS model 539) in degassed water.

The complete data were passed to a collection of aberration-correction codes implementing OFF and three comparison algorithms [5, 7, 8] (see [6] for implementation details). Each algorithm was given a list of target regions of interest (ROIs). The resulting set of estimated aberration profiles was then used to form corrected images of the phantom. The results shown in Fig. 3 were obtained using a 3-mm-thick aberrator with 1-mm-high ripples having a correlation length of 2.4 mm. A 6-mm gap was left between the transducer and the aberrator, which resulted in strongly azimuth-dependent aberration [6]. All six images share a common 0-dB reference.

In this comparison, OFF is the clear winner. (Examine the visibility of the deeper cysts, the definition of the shallower cysts, and the correction of the large extra-scattering cysts on the right-hand side.) The speckle brightness algorithm [8] performs well also. NFSR [5] and NNCC [7] are both hampered by an inability to find the correct aberration profiles at large angles from the array normal.

4. DISCUSSION AND CONCLUSIONS

Tissue-induced aberration is still a problem plaguing medical ultrasound imaging. Solutions based on single-valued focusing operators may not be sufficient to restore diffraction-limited resolution in all cases, but our results clearly demonstrate that significant improvement over published algorithms is possible.

The proposed algorithm is very similar to the approach described by Taner et al. for the seismic statics problem [9], the key addition being the angle-selectivity afforded by fan filtering. Like the linear system described in that work, the $\mathbf{A}$ matrix in OFF turns out to be rank-deficient. In this formulation, the rank is always $N-2$, implying that the solution for τ is indeterminate by a linear component. This is not a problem in practice, because the linear component is small and, to first order, equivalent to a change in focusing depth or steering angle.

The effect of iteration on OFF remains to be investigated. In cases of severe aberration, a partially correct estimated profile from the first iteration could be applied to the raw data prior to the second iteration. Correcting some or most of the aberration prior to fan filtering would reduce the spreading effect of aberration in spatial frequency, possibly leading to a better aberration estimate.

The complete data sets and MATLAB code used for this research are freely available at the Bioacoustics Research Lab web site, `http://www.brl.uiuc.edu/`.

5. ACKNOWLEDGEMENTS

The support of many people in the Bioacoustics Research Lab have made this research project a success; in particular, the authors thank Jim Blue, Dennis Matthews, Rita Miller, and Mark Johnson for their assistance with the experimental work. Many helpful suggestions and critiques were given by Joseph Dellinger and his colleagues in BP's Upstream Technology Group, by Yue Li, and by Andrew Paplinski.

6. REFERENCES

[1] A. J. Berkhout, "Pushing the limits of seismic imaging, Part I: Prestack migration in terms of double dynamic focusing," *Geophysics*, vol. 62, no. 3, pp. 937–953, May–June 1997.

[2] D. Rachlin, "Direct estimation of aberrating delays in pulse-echo imaging systems," *J. Acoust. Soc. America*, vol. 88, no. 1, pp. 191–198, July 1990.

[3] Y. Li, D. Robinson, and D. Carpenter, "Phase aberration correction using near-field signal redundancy," *IEEE Trans. UFFC*, vol. 44, no. 2, pp. 355–379, March 1997.

[4] J. F. Claerbout, *Imaging the Earth's Interior*. Palo Alto, CA: Blackwell Scientific Publications, 1985.

[5] Y. Li and B. Robinson, "Small element array algorithm for correcting phase aberration using near-field signal redundancy," *IEEE Trans. UFFC*, vol. 47, no. 1, pp. 29–57, January 2000.

[6] M. A. Haun, "New approaches to aberration correction in medical ultrasound imaging," Ph.D. dissertation, University of Illinois at Urbana-Champaign, 2003. [Online]. Available: http://angwin.csl.uiuc.edu/~haunma/work/

[7] S. W. Flax and M. O'Donnell, "Phase-aberration correction using signals from point reflectors and diffuse scatterers," *IEEE Trans. UFFC*, vol. 35, no. 6, pp. 758–774, November 1988.

[8] L. Nock, G. E. Trahey, and S. W. Smith, "Phase aberration correction in medical ultrasound using speckle brightness as a quality factor," *J. Acoust. Soc. America*, vol. 85, no. 5, pp. 1819–1833, May 1989.

[9] M. T. Taner, F. Koehler, and K. A. Alhilali, "Estimation and correction of near-surface time anomalies," *Geophysics*, vol. 39, no. 4, pp. 441–463, August 1974.

For $s = 1 \ldots N$ {

Filter $d_g(t; s)$ with fan filter passing angles $\rho \pm \Delta\rho$, where $\rho = \arctan\left(\frac{x_{\mathrm{ROI}} - x_s}{z_{\mathrm{ROI}}}\right)$.

}

For $m = 1 \ldots N$ {

For $h = h_{min} \ldots h_{max}$ {

Interpolate $d_{m+h,m-h}(t) \;\rightarrow\; d_{m+h,m-h}(t')$ using (4).

}

For $h_1 = h_{min} \ldots h_{max}$ {

For $h_2 = (h_1 + 1) \ldots h_{max}$ {

Cross-correlate $d_{m+h_1,m-h_1}(t')$ and $d_{m+h_2,m-h_2}(t')$ at lags $-\Delta_{max} \ldots \Delta_{max}$, yielding shift estimate $\Delta_{h_1 h_2}$.

If peak correlation $> x_{thresh}$ {

$$\mathbf{A} = \begin{bmatrix} & & & & & & & & & & & & \mathbf{A} & & & & & & & & & & & \\ \cdots & 0 & \overset{(m-h_2)}{-1} & 0 & \cdots & 0 & \overset{(m-h_1)}{1} & 0 & \cdots & 0 & \overset{(m+h_1)}{1} & 0 & \cdots & 0 & \overset{(m+h_2)}{-1} & 0 & \cdots \end{bmatrix}$$

$$\mathbf{b} = \begin{bmatrix} \mathbf{b} \\ \Delta_{h_1 h_2} \end{bmatrix}$$

}

}

}

}

Regularize $\mathbf{A}$ and solve $\mathbf{A}\tau = \mathbf{b}$ using the singular-value decomposition.

Figure 2: Least-squares solution for the aberration profile at $(x_{\mathrm{ROI}}, z_{\mathrm{ROI}})$. The signals received after firing element s are denoted $d_g(t; s)$; x_s is the position of element s. After fan-filtering, common-midpoint signal sets are processed one midpoint at a time. h_{min} and h_{max} define the range of offsets to consider. $\Delta\rho$ must be large enough to pass signals at h_{max}.

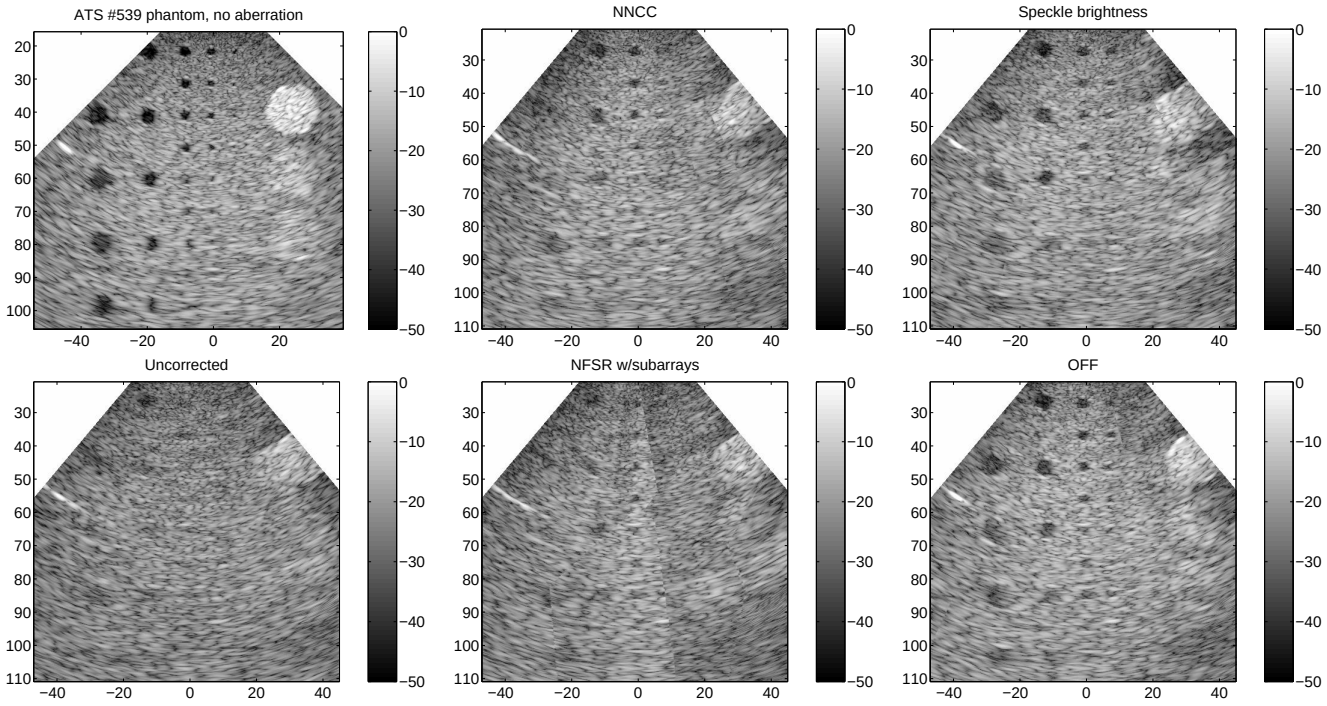

Figure 3: Images of data set ats_2ab1—original (data set ats), uncorrected, and corrected with aberration profiles supplied by four different algorithms. (Axis labels are in millimeters.)